Appl. Phys. B 80, 227–230 (2005)
DOI: 10.1007/s00340-004-1712-2

Applied Physics B
Lasers and Optics

U. HARTWIG[1]
K. PEITHMANN[2]
B. STURMAN[3]
K. BUSE[1,✉]

Strong permanent reversible diffraction gratings in copper-doped lithium niobate crystals caused by a zero-electric-field photorefractive effect

[1] Institute of Physics, Wegelerstraße 8, 53115 Bonn, Germany
[2] Helmholtz Institute for Radiation and Nuclear Physics, Nußallee 14–16, 53115 Bonn, Germany
[3] Institute of Automation and Electrometry, 630090 Novosibirsk, Russia

Received: 8 November 2004
Published online: 15 December 2004 •

ABSTRACT Permanent reversible diffraction gratings with refractive-index modulations of up to $\simeq 10^{-4}$ and with a grating vector perpendicular to the polar axis are realized in $LiNbO_3$:Cu crystals by making use of high temperature recording and charge compensation. The index changes do not result from light-induced space-charge fields and the linear electro-optic effect. They are linked to fixed high-contrast narrow-band absorption gratings of Cu^+/Cu^{2+} ions via the Kramers–Kronig relations.

PACS 42.65; 42.70; 72.40; 78.20

1 Introduction

A strong need for permanent and, at the same time, rewritable diffraction gratings exists in the area's holographic storage systems, narrow-band spatial filters, frequency converters, and laser feedback reflectors [1–4]. Photorefractive materials, such as lithium niobate crystals ($LiNbO_3$) or lithium tantalate crystals ($LiTaO_3$), offer great possibilities for reversible recording and addressable readout of optical information by making use of light-induced charge separation and the linear electro-optic effect [5, 6]. Unfortunately, the space-charge-field-induced electro-optic index gratings attributed to the classical photorefractive effect are usually volatile. They disappear upon homogeneous illumination or even in the dark.

Thermal fixing has been developed to make the charge gratings permanent [7, 8]. A light-induced redistribution of electrons between partially occupied deep traps by non-uniform photo-excitation is compensated by migration of thermally mobilized but optically passive ions, often H^+. In the final stage of recording, strong electronic and ionic charge gratings compensate each other almost completely. After cooling the crystal, the ions become immobile, and the recorded information cannot be erased with light. Lifetimes of several years have been demonstrated for thermally fixed holograms [7, 9, 10]. Erasure and rewriting of information can be accomplished with the help of thermal treatments.

✉ Fax: +49-228-734038, E-mail: kbuse@uni-bonn.de

In this paper we show that high-temperature recording and charge compensation allows one to build up strong refractive-index gratings ($n_K \simeq 10^{-4}$) of a different origin in photorefractive $LiNbO_3$:Cu crystals. These gratings experience no degradation, they exist with a zero-electric space-charge field. Furthermore, the electro-optic properties of lithium niobate crystals allow an interplay between the classical photorefractive and the zero-electric-field photorefractive gratings using the phenomenon of anisotropic diffraction [11].

2 Experimental results

2.1 *Holographic performance*

The samples used in our experiments are cut out of $LiNbO_3$ wafers, doped by Cu indiffusion, and annealed in a dry argon atmosphere [12]. The concentrations of the Cu^+ and Cu^{2+} ions can be directly determined by absorption measurements at the wavelengths $\lambda = 477$ and 1040 nm [13], respectively. The data presented in this subsection are obtained for a sample of dimensions of $x \times y \times z = 5.0 \times 0.98 \times 6.0\,\mathrm{mm}^3$. The total Cu concentration is $N_0 \simeq 4.2 \times 10^{19}\,\mathrm{cm}^{-3}$, and the concentration ratio for Cu^+ and Cu^{2+} valence states is $N^+/N^{2+} \simeq 0.84$.

The conditions of our experiments are as follows: Two extraordinarily polarized light beams of equal intensity, derived from an Ar^+ laser operating at 488 nm, are incident symmetrically onto the x, z-face of the sample to build up a grating of a period length $\Lambda \simeq 0.49\,\mu\mathrm{m}$ whose grating vector is perpendicular to the polar c axis, see Fig. 1a. Recording is performed at $T = 180\,^\circ\mathrm{C}$ for 22 hours. The stability of the light interference fringes is ensured by the use of an active stabilization technique [14]. The diffraction efficiency of the grating during recording is monitored with the help of an expanded Bragg-matched beam from a He-Ne laser ($\lambda_r = 632.8$ nm). An apparent saturation of this parameter serves as a signal for termination of the recording process.

After recording, the sample is cooled to room temperature, and the diffraction efficiency of the grating η, defined as the intensity ratio of the diffracted and incident probe beams, is measured at the wavelengths 477, 488, 496, 501, 514, and 633 nm.

Two different readout schemes have been used:

For the first one, Fig. 1b, the readout angle meets the condition of conventional isotropic Bragg diffraction. Incident

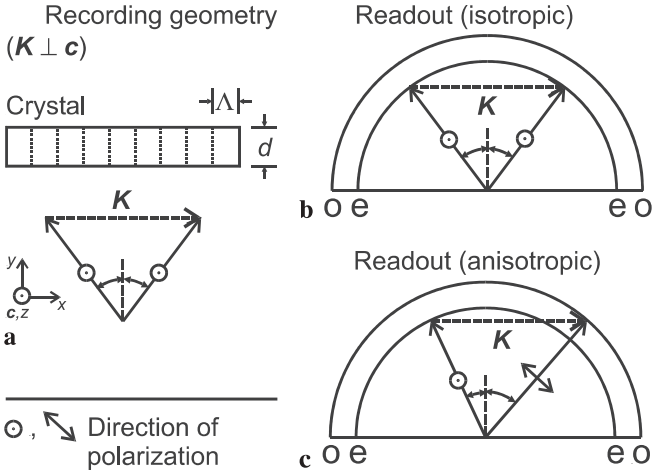

FIGURE 1 (**a**) Schematic illustration of the geometry for a recording experiment; the *dotted lines* show the grating fringes. (**b**) Wavevector diagram for isotropic diffraction. (**c**) The same for anisotropic diffraction

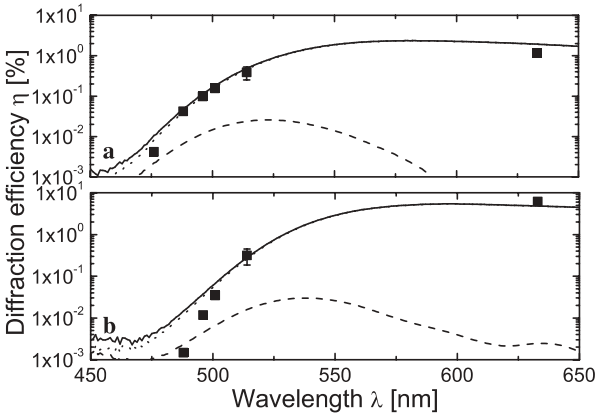

FIGURE 2 Spectral dependences of the diffraction efficiency for the extraordinarily (**a**) and ordinarily (**b**) polarized reading waves. The *squares* are experimental data, the *solid lines* show the best theoretical fit for $\eta(\lambda)$; the *dotted and dashed lines* are plotted for the contributions coming from the index and absorption gratings, respectively

and diffracted beams possess the same polarization, ordinary (o) or extraordinary (e), and the diffraction efficiency is given by $\eta^{\mathrm{o,e}} \simeq (\pi n_{\mathrm{K}}^{\mathrm{o,e}} d/\lambda_{\mathrm{r}})^2$, where $d = 0.98$ mm is the hologram thickness and $n_{\mathrm{K}}^{\mathrm{o,e}}$ is the amplitude of the refractive-index changes.

In the second scheme the readout beam (o or e) meets the condition of anisotropic diffraction [11]: $\sin\theta_{\mathrm{r}}^{\mathrm{o,e}} \simeq (\lambda_{\mathrm{r}}/2\Lambda)[1 \pm (\Lambda/\lambda_{\mathrm{r}})^2(n_{\mathrm{o}}^2 - n_{\mathrm{e}}^2)]$, see Fig. 1c. Here n_{o} and n_{e} are the refractive indices for ordinary and extraordinary light polarization, respectively. This diffraction is distinguished by a 90° change of the polarization angle; this is due to the light-induced change of the non-diagonal element of the optical permittivity tensor, $\varepsilon_{13,\mathrm{K}}$. The efficiency of the anisotropic diffraction is $\eta_{\mathrm{a}} \simeq (\pi\varepsilon_{13,\mathrm{K}} d/2\lambda_{\mathrm{r}})^2$. The photorefractive contribution $\varepsilon_{13,\mathrm{K}} \simeq n_{\mathrm{o}}^3 r_{51} E_{\mathrm{K}}$ is expected to dominate in our case because of the large electro-optic coefficient, $r_{51} \approx 30$ pm/V, of $LiNbO_3$ [15].

Isotropic diffraction. Experimental data on the spectral dependence of $\eta^{\mathrm{o,e}}$ are represented by squares in Fig. 2. The values of $\eta^{\mathrm{o,e}}$ experience no significant changes in the dark, and they cannot be erased optically.

The data cannot be explained by the presence of space-charge fields. Any index modulations $n_{\mathrm{K}}^{\mathrm{e}}$ resulting from the linear electro-optic effect are forbidden by symmetry. The values $n_{\mathrm{K}}^{\mathrm{o}} = (1-9)\times 10^{-5}$, observed in our experiments, exceed considerably the photorefractive contribution $\delta n_{\mathrm{K}}^{\mathrm{o}} = n_{\mathrm{o}}^3 r_{22} E_{\mathrm{K}}/2$. This holds true because the electro-optic coefficient r_{22} is smaller than 5 pm/V [15] in $LiNbO_3$, and the space-charge field amplitude E_{K} cannot exceed the characteristic diffusion field $(E_{\mathrm{K}})\mathrm{max} = Kk_{\mathrm{B}}T/e \approx 3$ kV/cm, where k_{B} is Boltzman's constant and e is the elementary charge.

Anisotropic diffraction. The maximum efficiency of anisotropic diffraction observed in our experiments, $\eta_{\mathrm{a}} \approx 0.1$, corresponds to the expected classical photorefractive value considering the maximum amplitude of the space-charge field, $(E_{\mathrm{K}})_{\mathrm{max}} \approx 3$ kV/cm. Furthermore, the value of η_{a} experiences remarkable changes during the dark decay-development cycle.

2.2 *Concentration measurements*

The samples used in the concentration measurements are prepared like the samples used in Sect. 2.1. A sample of the dimensions of $x \times y \times z = 5.0 \times 1.0 \times 6.0\,\mathrm{mm}^3$ is studied. The total Cu concentration of the sample is $N_0 \simeq 6.0 \times 10^{19}\,\mathrm{cm}^{-3}$, and the concentration ratio for Cu^+ and Cu^{2+} valence states is $N^+/N^{2+} \simeq 1.0$. A light pattern with a Gaussian-shaped intensity distribution in z-direction ($1/e^2$ width ~ 0.6 mm) and homogeneous intensity distribution in x-direction is used to record a macroscopic absorption pattern in the crystal at 180 °C (see [8] for details). The absorption measurements are preformed utilizing a Varian Cary 500 spectrometer. A slit aperture (width 100 μm) is placed in the signal path of the spectrometer in front of the sample. The crystal itself is placed on a translation stage and can be shifted parallel to its c axis inside the spectrometer. From the measurements of the absorption, the local concentrations of Cu^+ and Cu^{2+} centers are obtained [13].

Figure 3 shows the concentration of Cu^+, and Cu^{2+}, as well as the total Cu concentration vs. the spatial coordinate x of the crystal. The concentrations are represented by dashed, dotted, and solid lines, respectively. A strong variation of the Cu^+ and Cu^{2+} concentrations is clearly seen in the illuminated area, but the total Cu concentration is nearly constant throughout the sample.

2.3 *Photo-excitation cross-section measurements*

To determine the photo-excitation cross-sections, we measure the absorption spectra of the sample introduced in Sect. 2.1 ($N_0 = 4.2 \times 10^{19}\,\mathrm{cm}^{-3}$) for different oxidation/reduction states (different ratios of N^+/N^{2+}) with no grating recorded. The Cu^+ and Cu^{2+} ions are responsible for the absorption bands centered at $\lambda \approx 380$ and 940 nm, respectively [12, 13]. By making sure that the absorption changes for the low- and high-energy bands are proportional to N^+ and N^{2+}, respectively, we were able to calculate the spectra of the photo-excitation cross-section of the Cu^+ and Cu^{2+} centers, $\sigma_{\mathrm{o,e}}^{+}$ and $\sigma_{\mathrm{o,e}}^{2+}$. The subscripts o and e refer, as earlier, to the ordinary and extraordinary polarization. The corresponding

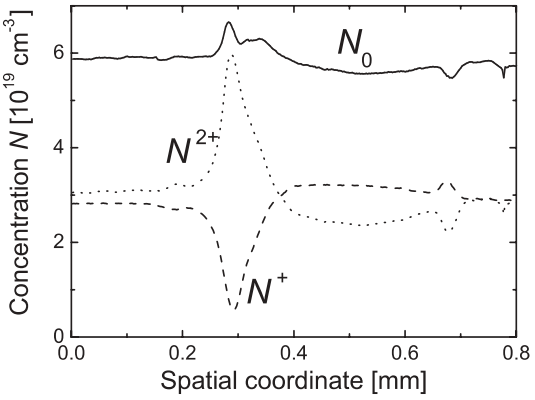

FIGURE 3 Concentration of Cu centers versus the spatial coordinate along the *c* axis after high-temperature recording of a macroscopic Gaussian intensity pattern; *dashed, dotted, and solid lines* show the Cu^{+}, Cu^{2+}, and total Cu concentration profiles, N^{+}, N^{2+}, and N_0, respectively

results are presented in Fig. 4. The part of the photo-excitation cross-section spectra $\sigma^{+}_{o,e}$ for wavelengths below 320 nm, not shown in the figure, could not be measured reliably because of the proximity of the fundamental absorption edge. This drawback does not affect significantly the subsequent results.

3 Discussion

The findings presented in Sect. 2.1 show unambiguously that the recorded grating possesses a permanent part of a non-classical photorefractive origin, which is dominating during isotropic readout, and a non-permanent classical photorefractive part, which is the largest upon anisotropic readout.

From Fig. 3 it can be clearly seen that the distribution of the concentration of Cu is not affected by the recording process at high temperatures. This means that during high temperature holographic recording, Cu ions do not move inside the crystal. Therefore the zero-electric-field photorefractive effect can not be explained by a spatial modulation of Cu ions themselves.

To explain the observed zero-electric-field photorefractive effect, we take a close look at the absorption spectra of Cu^{+} and Cu^{2+} ions representing the optically excitable species in $LiNbO_3$:Cu. A strong spatial modulation of the Cu^{+} and Cu^{2+}

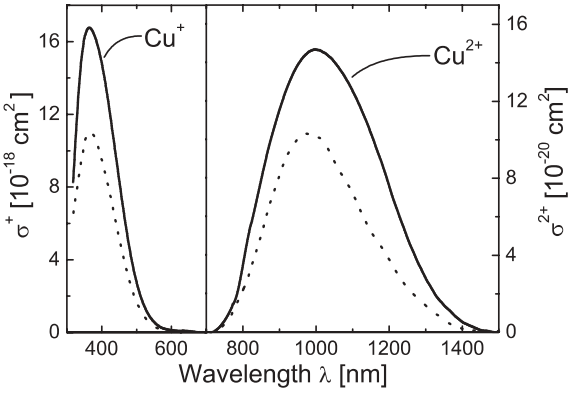

FIGURE 4 Spectral dependences of the photo-excitation cross-sections for Cu^{+} and Cu^{2+} centers; *solid and dotted lines* are plotted for o and e polarized light, respectively

concentrations is obtained upon thermal fixing [8]. This yields an absorption grating. The key point is that such an absorption grating is linked, over a pretty large spectral range, to a refractive-index grating via the Kramers–Kronig relations.

With the known absorption properties of Cu^{+} and Cu^{2+} centers (Fig. 4), we can describe quantitatively the spectral dependences of the amplitudes of the absorption and index gratings (α_K and n_K) for the thermally fixed hologram, as well as the dependence $\eta(\lambda)$. Since the total concentration of Cu is constant across the sample, we can write for the partial modulation amplitudes $N^{+}_{K} = -N^{2+}_{K}$. Therefore the spectral dependence of the absorption grating amplitude is given by $\alpha_K(\lambda) = N^{+}_{K}[\sigma^{+}(\lambda) - \sigma^{2+}(\lambda)]$. The amplitude of the refractive index changes, n_K, can be found from the Kramers–Kronig relation [16],

$$n_K = \frac{c}{\pi} P \int_0^{\infty} \frac{\alpha_K(s)}{s^2 - \omega^2}\, \mathrm{d}s\,, \tag{1}$$

where P stands for the principal value of the integral, ω is the light frequency, and s is the frequency over which the absorption modulation α_K is integrated. The only fit parameter in the relations for $\alpha_K(\lambda)$ and $n_K(\lambda)$ is the concentration amplitude N^{+}_{K}.

The solid lines in Fig. 2a,b show the dependences $\eta^{o,e}(\lambda)$ calculated for $N^{+}_{K} = 2.3 \times 10^{18}\ \mathrm{cm}^{-3}$, which gives the best fit. One sees that the agreement between theory and experiment is pretty good in the whole investigated spectral range. The direct changes of the optical permittivity, caused by the concentration Cu^{+}/Cu^{2+} grating, are thus responsible for the light diffraction. The permanent grating generally consists of phase and absorption components. The corresponding contributions to $\eta^{o,e}$ are shown by the dotted and dashed lines, respectively. Apart from the short-wavelength range, $\lambda \lesssim 500$ nm, and especially in the infrared range, the index grating is clearly dominating.

Several other issues relevant to the effect in question are worth of attention:

A zero-electric-field photorefractive effect reported in KTN and KLTN mixed crystals [17] is explained by strain-coordinated Jahn–Teller relaxations [18]. Lithium niobate crystals possess a higher stiffness and less lattice defects. In accordance with our data, the zero-electric-field effect has an entirely different origin here. Furthermore, this effect is at least one order of magnitude stronger as compared to that in KTN and KLTN crystals.

The first observation of unusual permanent gratings has been reported for $LiNbO_3$:Ti:Cu channel waveguides in 2001 [19]. The mechanism of this effect remained unclear. It is fully explained by the model considered in this paper.

First experiments have shown that similar effects occur in lithium niobate crystals doped with Fe during high temperature recording. However, for doping levels smaller than $2 \times 10^{19}\ \mathrm{cm}^{-3}$, that are optimum for photorefractive applications, it is less pronounced than in Cu-doped samples, because of different absorption spectra of $Fe^{2+/3+}$ and $Cu^{+/2+}$ in $LiNbO_3$.

The experimentally found contrast of the Cu^{+} grating, $N^{+}_{K}/N^{+} \approx 1/8$, can, most likely, be increased up to about one

by decreasing the grating period or/and increasing the recording time [20]. This would bring us to an amplitude of the index changes of $n_K \approx 7 \times 10^{-4}$.

4 Conclusion

We have shown that permanent diffraction gratings can be recorded at high temperatures in x and y cut lithium niobate crystals doped with Cu. Changes of the absorption coefficient, that result from a spatial modulation of Cu^+/Cu^{2+} centers and lead to strong modulations of the refractive index via the Kramers-Kronig relations, are responsible for polarization-isotropic diffraction in a wide range of wavelengths.

ACKNOWLEDGEMENTS Financial support from the Deutsche Telekom AG and from the DFG (FOR 557) is gratefully acknowledged.

REFERENCES

1 H.J. Coufal, D. Psaltis, G.T. Sincerbox (eds.), *Holographic Data Storage* (Springer 2000)
2 P. Boffi, D. Piccinin, M.C. Ubaldi (eds.), *Infrared Holography for Optical Communications*, Vol. 86 of Topics in Applied Physics (Springer 2003)
3 M. Centini, C. Sibilia, M. Scalora, G. D'Aguanno, M. Bertolotti, M.J. Bloemer, C.M. Bowden, I. Nefedov: Phys. Rev. E **60**, 4891 (1999)
4 S. Yiou, F. Balembois, P. Georges, J.P. Huignard: Opt. Lett. **28**, 242 (2003)
5 L. Solymar, D.J. Webb, A. Grunnet-Jepsen: *The Physics and Applications of Photorefractive Materials* (Claredon Press, Oxford 1996)
6 K. Buse: Appl. Phys. B **64**, 273 (1997)
7 J.J. Amodei, D.L. Staebler: RCA Rev. **33**, 71 (1972)
8 K. Buse, S. Breer, K. Peithmann, S. Kapphan, M. Gao, E. Krätzig: Phys. Rev. B **56**, 1225 (1997)
9 L. Arizmendi, E.M. de Miguel-Sanz, M. Carrascosa: Opt. Lett. **23**, 960 (1998)
10 E.M. de Miguel-Sanz, M. Carrascosa, L. Arizmendi: Phys. Rev. B **65**, 165 101 (2002)
11 P. Günter, J.P. Huignard (eds.), *Photorefractive Materials and Their Applications, II*, Vol. 62 of Topics in Applied Physics (Springer-Verlag, Berlin 1982) Chapt. 1
12 K. Peithmann, J. Hukriede, K. Buse, E. Krätzig: Phys. Rev. B **61**, 4615 (2000)
13 E. Krätzig, R. Orlowski: Ferroelectrics **27**, 241 (1980)
14 S. Breer, K. Buse, K. Peithmann, H. Vogt, E. Krätzig: Rev. Sci. Instrum. **69**, 1591 (1998)
15 M. Jazbinšek, M. Zgonik: Appl. Phys. B **74**, 407 (2002)
16 J.D. Jackson: *Classical Electrodynamics* (John Wiley & Sons, New York 1999)
17 A. Agranat, V. Leyva, A. Yariv: Opt. Lett. **14**, 1017 (1989)
18 R. Hofmeister, A. Yariv, S. Yagi, A. Agranat: Phys. Rev. Lett. **69**, 1459 (1992)
19 J. Hukriede, D. Kip, E. Krätzig: Appl. Phys. B **72**, 749 (2001)
20 B. Sturman, M. Carrascosa, F. Agulló-López, J. Limeres: Phys. Rev. B **57**, 12 792 (1998)